

Damping estimation of offshore wind turbines using state-of-the art operational modal analysis techniques

M. El-Kafafy¹, C. Devriendt¹, G. De Sitter¹, T. De Troyer^{1,2}, P. Guillaume¹

¹Vrije Universiteit Brussel - Acoustics & Vibration Research Group
Pleinlaan 2, B-1050 Brussel, Belgium
e-mail: melkafaf@vub.ac.be

²Erasmushogeschool Brussel
Nijverheidskaai 170, B-1070 Brussel, Belgium

Abstract

In this paper, one existing modal analysis tool together with recently proposed modal parameter estimation approaches [1, 2] will be investigated with respect to their applicability to identify the damping values of an offshore wind turbine and compared with the traditional log-decrement approach. The experimental data has been obtained during a measurement campaign on an offshore wind turbine in the Belgian North Sea in the framework of the Flemish funded off shore wind infrastructure project. Real damping ratios are very difficult to predict by numerical tools and therefore measurements on existing offshore wind turbines are crucial to verify the design assumptions in estimating the lifetime of an offshore wind turbine.

It will be shown that damping ratios can directly be obtained from vibrations of the tower under ambient excitation from wave and wind loading. The results will be compared with the approach that is used nowadays to determine the damping of offshore wind turbines: an overspeed emergency stop followed by a logarithmic decrement analysis. An emergency stop, however, reduces the remaining lifetime of the wind turbine. The frequency-domain OMA techniques, presented in this paper, do not require emergency stops, which is clearly an economic advantage and a more practical approach. The advanced modal analysis tools, which will be investigated, include the poly-reference Least Squares Complex Frequency-domain estimator (pLSCF) - commercially known as PolyMAX - estimator and two newly proposed modal estimation approaches [1, 2]. The newly proposed modal estimation approaches are a combination of the maximum likelihood estimator (MLE) and the pLSCF estimator. The advantage of these approaches is that they keep the benefits of the pLSCF estimator (e.g. very clear stabilization chart) while adding MLE features like improved estimates and proper handling of the measurement uncertainties.

1 Introduction

Damping plays a key role in the dynamic design of engineering structures, especially for response prediction and vibration control, as well as in structural health monitoring. The dynamic response of a structure is determined by the dynamic characteristics of the structure and the external loads. Resonance plays a key role in the dynamic response especially for a lightly damped structural system. Two critical parameters of a resonance are the resonance frequency and the damping ratio, which are determined by mass, stiffness and damping characteristics of the system. In mechanical and civil engineering, structures are often subjected to broadband excitation, such as turbulence, wind, sea waves, traffic, etc. In this case, damping has a critical influence on the dynamic response and the lack of the damping is the main reason for excessive vibration in the structural system.

Indeed, offshore wind turbines are considered as structures whose dynamic characteristics are heavily affected by the ambient excitations. To determine the real damping of offshore wind turbines, modal testing should be applied. Modal parameters of any vibratory structure can be identified using very simple techniques like log-decrement, exponential decay least squares fitting and half-power bandwidth methods

which are still commonly used because they are simple and fast, and they yield accurate results if the damping is low and the modal frequencies of interest have sufficient separations among them [3, 4]. These approaches, which are considered as single degree of freedom (SDOF) approaches, can be used to deal with operational analysis where it can be applied to either the free vibration decay in case of using the log-decrement and exponential decay fitting methods or the power and cross-spectral densities of the operational responses in case of using the half-power bandwidth method. In the class of MDOF algorithms, a major grouping is usually done based on the domain in which the data are treated numerically resulting in time-domain and frequency domain methods.

Regarding with modal parameter identification in the frequency-domain, there are many modal parameter estimation (MPE) algorithms that start from the frequency response functions or the outputs power spectra. The frequency-domain techniques can be classified into two categories, deterministic approaches and stochastic approaches. Some popular estimators in the deterministic framework are the Least Squares Complex Frequency-domain (LSCF) estimator and its poly-reference version, the pLSCF estimator – commercially known as PolyMAX- [5, 6, 7]. The main advantages of these estimators are the fastness and their clear stabilization chart. In [8], the pLSCF estimator was applied to output-only measured data and it was compared to the correlation-driven stochastic subspace identification approach. Although both pLSCF and the stochastic subspace algorithm approximately yield the same modal parameter estimates, the results show that the operational pLSCF results in a more clear stabilization chart and it is easier to automate than the stochastic subspace algorithm. Recently a complete new OMA approach, based on the transmissibility measurements, was proposed [9]. This approach does not require the assumption that the forces are white noise sequences and in [10], it is shown that this technique can deal with harmonics when the loads are correlated.

In the stochastic framework, the major breakthrough was the development of the Maximum Likelihood estimator (MLE) introduced in [11] where the modal parameters were estimated in a maximum likelihood sense for the first time. This estimator outperforms the classical deterministic techniques in terms of the estimate accuracy. Moreover, it delivers the confidence bounds on the estimated parameters. The applicability of this estimator in the field of output-only modal analysis is investigated in [12] and the results were very promising. In [1, 2], it was shown that by combining the stochastic and deterministic approaches one can get the best features of both approaches where we can have a clear stabilization chart in a fast way together with accurate modal parameters estimates. A combined ML-pLSCF approach – commercially known as the PolyMAX Plus- is introduced in [1]. In this approach, the noisy measured data are firstly smoothed in a maximum likelihood sense to remove the noise without missing any information from the data and then in a second step the classical pLSCF estimator is applied to the smoothed data to have a clear stabilization chart with accurate estimates.

The results from this approach show that it outperforms the classical pLSCF estimator especially for the cases where the data is either very noisy or containing poorly excited modes. In [2], another combination between the stochastic and deterministic approaches was introduced. In this approach, a maximum likelihood estimator (ML-MM) was introduced but it uses a parameterization form, that differs from the one used by the classical MLE, i.e. it works directly with the modal model form rather than the rational fraction polynomial parameterization. To have initial values for the modal model parameter, we apply the classical pLSCF estimator followed by the LSFD estimator. By doing so, the initial values estimated by the pLSCF –LSFD estimators can be further improved, moreover the uncertainty on these improved estimates is delivered directly without using many linearization formulas [13] like in the classical ML-estimator. As we see, many techniques can be used to extract the modal parameters from the measured data in the modal testing process. When we apply these techniques to an operational offshore wind turbine, we find that the situation is very complex. During the operation of the offshore wind turbine (OWT), there are rotating components that correspond with harmonic forces and wind – wave interaction with the structure. These reasons make the offshore wind turbine to fail to comply the OMA assumptions.

In the present contribution, the applicability of three classical modal parameter estimation techniques will be studied to estimate the damping of the 1st tower mode of operational offshore wind turbine. These

techniques are the pLSCF estimator, the combined ML-pLSCF estimator, and the ML-MM estimator. The damping will be estimated using two different measured datasets. The first data set is obtained by performing an overspeed test where we can have the free-decay response of the OWT. The second data set is a 40 minutes acceleration response record due to ambient excitations measured where the OWT is slowly rotating.

2 Applied Identification Techniques

2.1 Polyreference LSCF (PolyMAX)

It is known that the frequency response functions and the positive power spectra-also known as half power spectra- can be parameterized in exactly the same way [8]. By consequence, the pLSCF estimator [6], which is normally applied to FRF data, can be applied to the outputs positive power spectra in case of OMA. In the pLSCF method, the following so-called right matrix fraction model is assumed to represent the measured positive power spectrum matrix of the outputs:

$$S_{yy}^+(\omega_k) = \sum_{r=0}^n \Omega^r [\beta_r] \cdot \left(\sum_{r=0}^n \Omega^r [\alpha_r] \right)^{-1} \in \mathbb{C}^{N_o \times N_{ref}} \quad (1)$$

where $[\beta_r] \in \mathbb{R}^{N_o \times N_{ref}}$ are the numerator matrix polynomial coefficients; $[\alpha_r] \in \mathbb{R}^{N_{ref} \times N_{ref}}$ are the denominator matrix polynomial coefficients; n is the model order; N_o is the number of measured output signals; N_{ref} is the number of response DOFs taken as references. The pLSCF estimator uses a discrete time frequency domain model (z-domain model) with $\Omega = e^{-j\omega_k T_s}$ (ω_k is the circular frequency in radian and T_s is the sample time). Equation (1) can be written for all the values of the frequency axis of the positive power spectra data. Basically, the unknown model coefficients $[\beta_r]$ and $[\alpha_r]$ are then found as the least squares solution of these equations. Once the denominator coefficients $[\alpha_r]$ are determined, the poles λ_i and the modal reference factors $L_i \in \mathbb{C}^{N_{ref} \times 1}$ are retrieved as the eigenvalues and eigenvectors of their companion matrix [14, 6]. An n^{th} order right matrix-fraction model yields nN_{ref} poles. As we mentioned in the introduction, this estimator gives a very clear stabilization chart in a fast way. Once we have the poles and the modal reference factors, the mode shapes together with the lower and upper residual terms can be obtained as the least squares solution of equation (2)

$$S_{yy}^+(\omega_k) = \frac{LR}{j\omega_k} + j\omega_k UR + \sum_{i=1}^{N_m} \frac{\Psi_i L_i^T}{j\omega_k - \lambda_i} + \frac{\Psi_i^* L_i^{*T}}{j\omega_k - \lambda_i^*} \in \mathbb{C}^{N_o \times N_{ref}} \quad (2)$$

where N_m is the number of modes selected from the stabilization chart; $\Psi_i \in \mathbb{C}^{N_o \times 1}$ is the i^{th} mode shape, and LR and UR are the lower and upper residual terms to model the effects of the out of band modes. It can be seen from equation (2) that the mode shapes, lower residuals and upper residuals are the only unknowns in this equation. So they can be easily obtained as the least squares solution of this equation. This method is commonly known in the field of modal analysis as LSF method [5, 6].

2.2 Combined ML-pLSCF (PolyMAX Plus)

This approach [1] is a combination between a stochastic approach (i.e. maximum likelihood estimator) and a deterministic approach (i.e. pLSCF estimator). It is proposed to overcome the drawback of the classical pLSCF. The drawback of the classical pLSCF estimator is that it gives unreliable damping estimates when

the noise level is high like the case of having inflight measurements or when the estimated modes are weakly excited. This approach consists of two steps, the second step is exactly the classical pLSCF estimator introduced in the subsection 2.1. In the first step, the noise on the data is eliminated by applying a global smoothing on the measured data in a maximum likelihood sense without missing any information from the original measured data. Since the noise is removed from the data in the first step, pLSCF in the second step works very well and gives very accurate estimates.

So in this subsection, we are going to show only and briefly the first step in this approach since the second step is already introduced in the subsection 2.1. In this approach, the Maximum likelihood estimator introduced in [11] is used in the first step to perform the data smoothing. The basic equations of this ML solver will be briefly recapitulated. The ML-estimator, introduced in [11], uses a rational fractional common denominator polynomial parameterization to model the frequency response functions. So the same parameterization can be used to model the positive auto/cross power spectrum matrix in case of output-only measurements:

$$\hat{S}_{yy_{oi}}^+(\omega_k) = \frac{\sum_{r=0}^n \Omega^r B_{oi_r}}{\sum_{r=0}^n \Omega^r A_r} \in \mathbb{C}^{1 \times 1} \quad (3)$$

with $i = 1, \dots, N_{ref}$; $o = 1, \dots, N_o$; $B_{oi_r} \in \mathbb{R}^{1 \times 1}$ the numerator polynomial coefficient for output –input combination oi at order r ; A_r is the denominator coefficient at order r and $\Omega = e^{-j\omega_k T_s}$. One can see that the numerator coefficients are different for each element of the outputs power spectrum matrix while the denominator coefficients are the same for each element. The coefficients $A \in \mathbb{R}^{n+1 \times 1}$ and $B \in \mathbb{R}^{(n+1)N_o N_{ref} \times 1}$ are the parameters to be optimized and estimated during the smoothing step (they will be represented by the parameter vector θ in the sequel of this section). Assuming the measured positive auto/cross power spectra functions $S_{yy_{oi}}^+(\omega_k)$ to be complex normally distributed and mutually uncorrelated, the (negative) log-likelihood function reduces to:

$$\ell_{ML}(\omega_f, \theta) = \sum_{k=1}^{N_o N_i} \sum_{f=1}^{N_f} \frac{|\hat{S}_{yy_{oi}}^+(\theta, \omega_k) - S_{yy_{oi}}^+(\omega_k)|^2}{var(S_{yy_{oi}}^+(\omega_k))} \quad (4)$$

where $var(S_{yy_{oi}}^+(\omega_k))$ is the variance of the positive power spectra of the outputs. If these data variances are not available from the measurements, they can still be estimated using the residual errors information (i.e. the difference between $\hat{S}_{yy_{oi}}^+(\theta, \omega_k)$ and $S_{yy_{oi}}^+(\omega_k)$) as it was demonstrated in [15]. The data smoothing is obtained by minimizing the cost function shown in equation (4). This can be done by means of a Gauss-Newton optimization algorithm which takes the advantage of the quadratic form of the cost function (4). After convergence, the estimated positive auto/cross power spectra functions, $\hat{S}_{yy_{oi}}^+(\theta, \omega_k)$, will perfectly fit the measured one, $S_{yy_{oi}}^+(\omega_k)$, which means that the estimated positive auto/cross power spectra functions, $\hat{S}_{yy_{oi}}^+(\theta, \omega_k)$, contains all the physical modes but with the benefit of the noise free compared to the measured positive auto/cross power spectra functions, $S_{yy_{oi}}^+(\omega_k)$. Therefore, applying pLSCF estimator in the second step on $\hat{S}_{yy_{oi}}^+(\theta, \omega_k)$ instead of $S_{yy_{oi}}^+(\omega_k)$ enables us to have more accurate modal parameter estimates together with a clear stabilization chart.

2.3 ML-MM estimator

This estimator, introduced in [2], is a combination between a deterministic and stochastic approach. The objective of this approach is to have the benefits of the pLSCF estimator of having a clear stabilization chart in a fast way, which is considered nowadays as a very popular assistance tool in the modal analysis field, and at the same time to deliver accurate modal parameters estimates together with their confidence

bounds. This approach consists of two steps. In the first step, preliminary modal parameter (i.e. poles, modal reference factors, mode shapes lower and upper residual terms) estimation process is done by applying the pLSCF estimator, introduced in subsection 2.1, on the measured data. Then, the stabilization chart is constructed and the poles with the modal reference factors are estimated. Then using the LSFD method the mode shapes, lower and upper residual terms are estimated in a least squares sense using equation (2). In the second step, the modal model given by equation (2) is started to be optimized in a maximum likelihood sense. At the end, we have a maximum likelihood estimator but with a different parameterization where the modal model is used instead of the classical rational fraction common denominator polynomial model which is used in the classical MLE in equation (3). The advantages of using this parameterization are firstly the physical modes selected from the stabilization chart are included only to the model so the effects of the mathematical poles can be eliminated. Secondly, the uncertainty on the modal parameters is delivered directly without using some linearization formulas like in the classical MLE. Under the same assumptions used for the classical MLE [11], the cost function of this estimator reduced to:

$$K_{ML}(\theta, \omega_f) = \sum_{o=1}^{N_o} \sum_{f=1}^{N_f} E_o^H(\theta, \omega_f) C_o^{-1}(\omega_f) E_o(\theta, \omega_f) \quad (5)$$

with H the complex, conjugate transpose of a matrix (Hermitian), $\theta = [\theta_{\psi_o} \ \theta_{LUR_o} \ \theta_L \ \theta_\lambda]^T$ where,

$$\begin{aligned} \theta_{\psi_o} &= [\psi_{o1} \ \psi_{o2} \ \dots \ \psi_{oN_m}], \\ \theta_{LUR_o} &= [LR_{o1} \ \dots \ LR_{oN_{ref}} \ \ UR_{o1} \ \dots \ UR_{oN_{ref}}], \theta_L = [L_1 \ L_2 \ \dots \ L_{N_m}], \\ \theta_\lambda &= [\lambda_1 \ \lambda_2 \ \dots \ \lambda_{N_m}] \end{aligned} \quad (6)$$

and the equation error (a column vector) given by

$$E_o(\theta, \omega_f) = S_{yy_o}^T(\omega_f) - \hat{S}_{yy_o}^T(\theta, \omega_f) \in \mathbb{C}^{N_{ref} \times 1} \quad (7)$$

where $\hat{S}_{yy_o}(\theta, \omega_f)$ represented by equation (2) for output o and $C_o(\omega_f) \in \mathbb{R}^{N_{ref} \times N_{ref}}$ is the covariance matrix of the equation error. This cost function is minimized by means of a Gauss-Newton optimization algorithm until convergence occurs. The implementation of this technique is optimized to decrease the computational time and memory requirements [2]. After convergence occurs, the uncertainty on the estimated modal parameters can be derived from the following equation [16]:

$$COV(\psi, LR, UR, L, \lambda) \approx [J^T J]^{-1} \quad (8)$$

where J is the Jacobian matrix calculated at the last iteration.

3 Offshore Measurements and Preliminary Analysis

As we mentioned before, two measurements campaigns were done. The second measurement campaign focused on performing an overspeed test with the aim of obtaining a first estimate of the damping value of the fundamental for-aft vibration mode of the wind turbine (i.e. 1st bending mode of the tower). The first measurement campaigns focused on performing 40 minutes vibration measurements due to the pure ambient vibration where the OWT rotor was slowly rotating. This ambient test was done just before the

overspeed test. The nacelle was put into the direction of the wind. The two measurement campaigns were performed at the Belwind wind farm. This wind farm is located in the North Sea on the Bligh Bank, 46 Km off the Belgian coast. The measurements are taken at four levels on nine locations using 10 sensors. The measurement locations are indicated in Figure 1 by yellow circles. The chosen sensors levels are at height of 52m, 22m, 8m, and 0m taken from the lower platform in the transitions piece. There are two accelerometers mounted at the lower three levels and four at the top level. The chosen configuration is primary aimed at identification of tower bending modes. The two extra sensors on the top level are placed to capture the tower torsion mode. During the measurement campaigns, discussed in this article, the sensors 7 and 8 were not yet installed. The objective in this paper is to estimate the additional offshore damping excluding the aerodynamic damping and the damping from damping devices. Therefore, during both the overspeed test and the ambient excitation test the tuned mass damper was turned off. For the overspeed stop test the wind speed was the minimum required 6.5m/s. This allows the wind turbine to speed up until 19.8 rpm. This is the speed at which the wind turbine is automatically stopped and the pitch angle is put on 88.2 degrees. First of all, a preliminary frequency domain analysis was carried out to identify the most relevant natural frequencies. To do so, the outputs power spectra are calculated for both the overspeed stop test data and the ambient excitation measured data. For the overspeed test, the Fast Fourier Transformation (FFT) of the free decays shown in Figure 2 is calculated for all the measured time records. Before calculating the FFT, we select only a segment from the total free decays as it is shown in Figure 2. For the ambient excitation test data, the Correlogram approach is used to calculate the outputs power spectrum and the pre-processing results are shown in Figure 3. A quick way to have a clue about the modes within the identified band is the stabilization chart tool. So, PolyMAX and PolyMAX Plus estimators were applied to the outputs spectra calculated from both overspeed stop and ambient excitations tests and we got the stabilization charts presented in Figure 4 and Figure 5. Inspection of these stabilization charts draws some remarks. First, one can clearly identify the dominant peak, which corresponds to the 1st bending mode of the tower (For-Aft mode), with a lot of other modes which correspond to the higher bending modes, blade modes and modes at lower frequencies ($<0.3\text{Hz}$) due to the wave excitations. Second, one can note that both the classical PolyMAX and the PolyMAX Plus estimators give a clear stabilization chart. That means introducing the smoothing step in the PolyMAX Plus does not affect the clarity of the stabilization chart. Third, a detailed inspection of the stabilization charts for the overspeed test (c.f. Figure 4) shows that PolyMAX Plus is more consistent than the classical PolyMAX where with varying the model order it gives more stable poles (i.e. poles with 's' symbol means that the variability in the estimated poles from order to another is lower). Moreover, by zooming around the dominant peak in the stabilization chart for the ambient vibration test (c.f. Figure 5), we can note that PolyMAX Plus is able to identify very close stable poles at the higher model order where classical PolyMAX does not.

At the vicinity of the dominant peak, PolyMAX and PolyMAX Plus identify only one mode around 0.35 Hz using the overspeed data while by using the ambient data set it has been noted that PolyMAX Plus identifies some other close modes at the vicinity of the dominant peak. The one at the peak corresponds to the 1st For-Aft (FA) mode while the other close modes correspond to the Side-to-Side movement of the tower. These modes are not visible in the stabilization chart of the overspeed test because the thrust release due to the sudden collective pitch variation excites the OWT tower mainly in the wind direction (c.f. Figure 1 direction of the sensors 1, 5, 7 and 9). Therefore, the movement of the OWT tower is dominant in the FA direction.

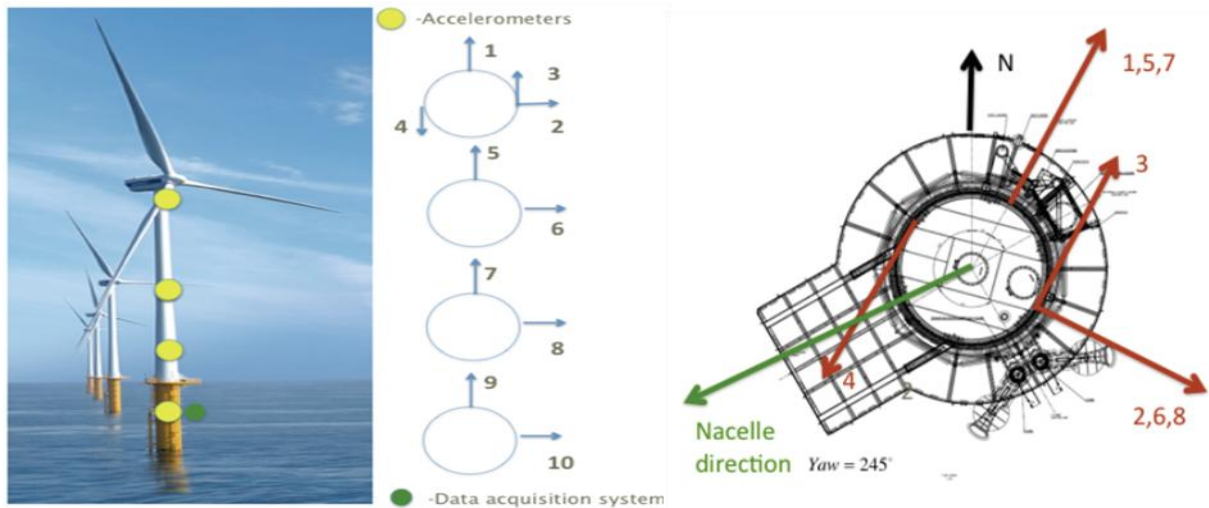


Figure 1: measurements locations

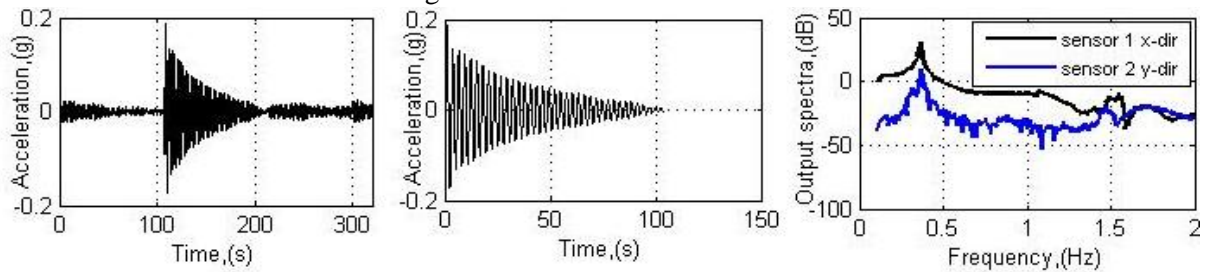


Figure 2: Overspeed stop test data processing (Left: full time record. Middle: selected segment. Right: Calculated Outputs spectra)

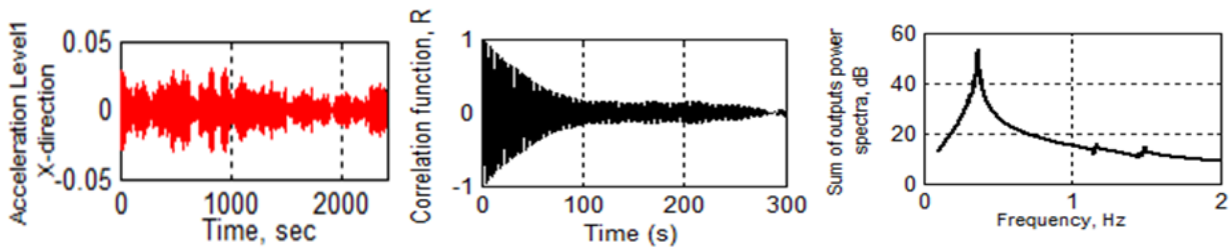


Figure 3: Ambient excitations test data processing (Left: 40 minutes time record. Middle: example of calculated correlation functions Right: sum of the calculated Outputs spectra)

From this comparison between the stabilization charts of the overspeed stop and ambient excitations tests, we can conclude that the 1st For-Aft (FA) mode and the 1st Side-to-Side mode have very close natural frequency values and the 1st FA mode occurs at a lower natural frequency than the SS mode. It seems from the spectrum of the measured signal that this mode (i.e. 1st FA mode) is the main vibration mode where the maximum vibration occurs. Therefore, the objective of this study is to identify the modal parameter (more specifically the damping ratio) of this fundamental OWT tower mode from the operational measurements (ambient excitations). This will help us to better understand the damping-effects in OWT and to better estimate the real lifetime of wind turbines. Therefore, in the following sections, we are going to track only the natural frequency and damping ratio of the 1st FA mode by applying the different estimators under test (i.e. PolyMAX, PolyMAX Plus and ML-MM) to the outputs auto/cross power spectra calculated from both the overspeed stop test and the ambient excitations test measurements. Before doing so, we are going to perform an exponential decay analysis on the time domain data obtained from the overspeed stop test to have a preliminary indication about the damping of that mode. The exponential decay fitting in time domain can give acceptable estimates for the damping if it is used in a proper way. A proper way means that the time domain signal should be dominant with one

mode. This simple method faces difficulties when the free decay signal contains several modes, e.g. 1st FA and 1st SS mode, with close frequencies or when the ambient force contributions are colored. In case the free decay contains several modes, it is recommended to filter the data using a band pass filter to isolate the mode under test from the other modes [3]. Since we are interested on the 1st bending mode of the OWT tower (i.e. 1st FA mode), we applied the exponential decay fitting to the measured accelerations of the sensors in the direction of the wind (i.e. Sensors 1, 5, and 9). The data was pre-filtered using 3 different band-pass filters. The fitting was performed between 0.8 and 0.2 of the maximum acceleration. The results are shown in Table 1. From Table 1, one can conclude that on one hand, the exponential decay fitting method may have some advantages like simplicity and fastness but on the other hand, its damping estimates depend on the sensor and the filter band to be used. The first filter band (i.e. .01-1.5Hz) seems to be incorrect since the fluctuation on the damping estimates from the different sensors is higher compared to the other filter bands. This is because this filter band allows several modes to contribute in the time-domain signal and hence makes it difficult to the exponential decay fitting to get a correct damping estimate. It is expected that the estimates using the narrow band-pass filter 0.3-0.5Hz around the frequency of the first FA mode are likely to be the most correct ones.

4 Damping Identification Using Different OMA Techniques

In this section, the applicability of the different frequency-domain estimators, presented in section 2, to estimate the damping of the 1st FA mode of the OWT will be studied. Note that these approaches fit a polynomial function with multiple modes to the measured data and therefore overcomes the limitations of the traditional procedure of fitting an exponential decaying function to the measured accelerations in the time domain. These approaches use advanced models that start from the idea that the overall vibration consists out of different modes. Therefore, their results are not affected by the fact that multiple modes are present in the measurements.

4.1 Overspeed Stop Test Data Analysis

In this subsection, the different estimators under test will be applied to the frequency-domain data obtained from applying an FFT to the free-decay time domain data (c.f. Figure 2). The stabilization charts constructed by each estimator (i.e. PolyMAX and PolyMAX Plus while the initial values for ML-MM are taken from the PolyMAX stabilization chart) are shown in Figure 4. From these stabilization charts, one can see clearly, as we mentioned before, that PolyMAX, and PolyMAX plus can identify a stable mode at the dominant peak which corresponds with the 1st FA mode around 0.35Hz.

Table 2 shows the estimated resonance frequency and damping ratio of the 1st FA mode using different techniques. In Figure 6, as an overall quality indicator of the parameter estimation process, the sum of the measured spectra is compared with the sum of the spectra that are synthesized from the identified modal parameters using equation (2). Figure 6 shows that PolyMAX Plus and ML-MM closely fit the measured spectra while PolyMAX does not especially in the higher frequency band (>0.8Hz). Zooming in around the dominant peak shows that ML-MM closely fits the maxima of the dominant peak compared with PolyMAX and PolyMAX Plus. In the same context, PolyMAX Plus fits the maxima of the dominant peak better than PolyMAX. The correspondence between measured and synthesized spectra by ML-MM and PolyMAX Plus estimators confirms the accuracy of their estimates.

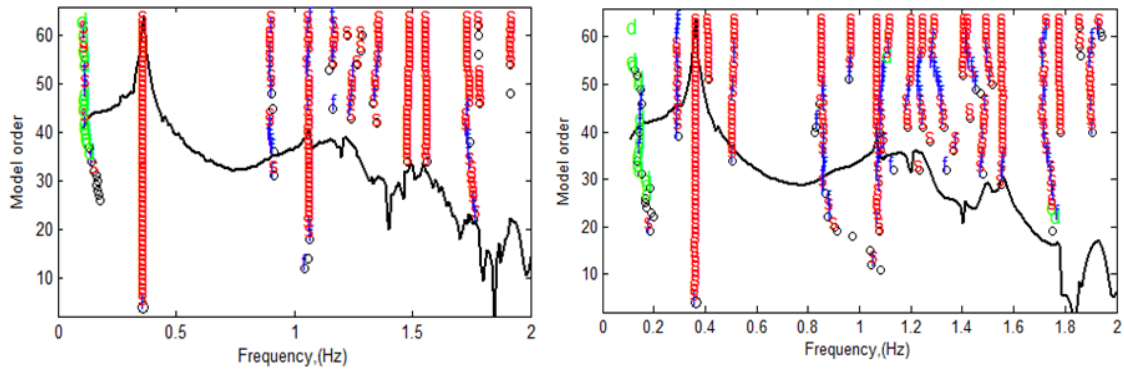


Figure 4: stabilization charts constructed by PolyMAX (left) and PolyMAX Plus (right) using outputs spectra calculated from the overspeed stop test

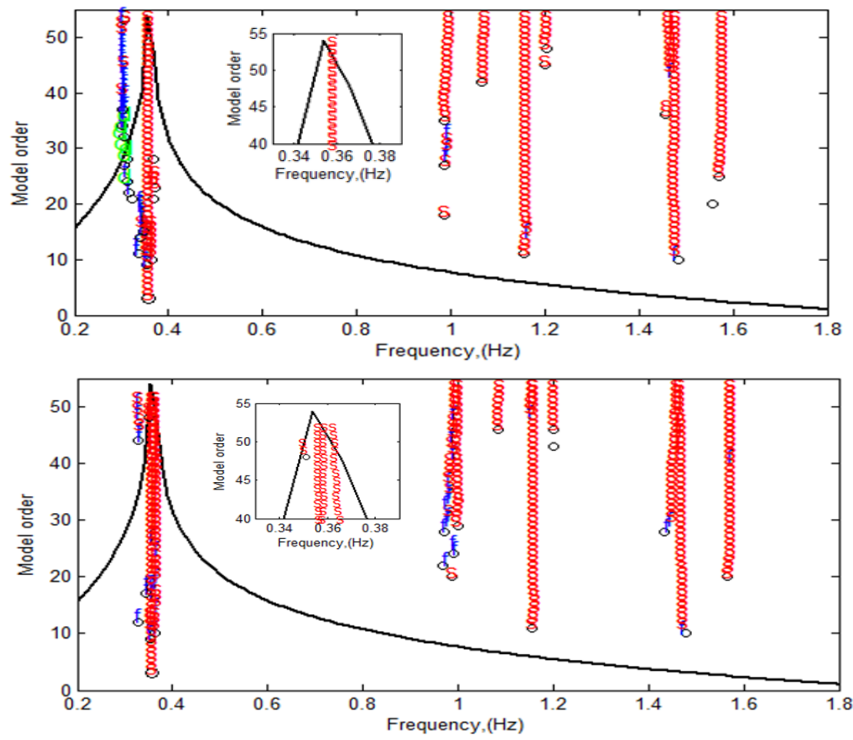


Figure 5: Stabilization charts constructed by PolyMAX (top) and PolyMAX Plus (bottom) using outputs spectra calculated from the ambient excitations test with zooming in around the dominant peak

Filter band / Sensor number	0.01-1.5Hz Filter 1	0.1-0.8Hz Filter 2	0.3-0.5Hz Filter 3
Sensor 1	1.1%	1.12%	1.04%
Sensor 5	0.98%	1.15%	1.05%
Sensor 9	0.86%	1.16%	1.05%

Table 1: Estimated damping ratios using different band-pass filters

	Natural frequency (Hz)	Damping ratio (%)
<i>PolyMAX</i>	0.351	1.014
<i>PolyMAX Plus</i>	0.3529	1.082
<i>ML-MM</i>	0.3523	1.089

Table 2: Estimated natural frequency and damping ratio for the 1st FA mode

4.2 Ambient Excitations Test Data Analysis

Ambient vibration tests have the strong advantage of being very practical and economical, as they use the freely available ambient wind and wave excitation. Furthermore, the data is collected during the normal use of the structure and consequently the identified modal parameters are associated with realistic vibration levels. In this subsection, we are going to apply the estimators under test on the outputs power spectra calculated from the measured accelerations due to purely ambient excitations. As we mentioned in section 3, we used the Correlogram approach to firstly calculate the auto and cross correlation functions taking the two sensors on the top (c.f. Figure 1) as reference signals. Then taking only the correlation functions having positive time lag and without applying exponential window, the positive (half) power spectra are calculated using the FFT.

From the preliminary analysis done in section 3, we noted that PolyMAX and PolyMAX Plus, when applied to the outputs power spectra, are able to identify a stable mode at the vicinity of the dominant peak around 0.35Hz (1st FA mode) like the case of the overspeed stop data set. In the following parts of this subsection, the natural frequency and the modal damping of this mode will be tracked using the different estimators under test. The parameters that have a stronger influence on the results are the length of the time segment taken from the full time record and the number of time lags taken from the correlation function used for the spectra calculation. The spectra resolution, controlled by the number of time lags taken from the correlation functions, should be high enough to well characterize all the modes within the selected frequency band. At the same time, it should be kept as low as possible to reduce the effect of the noise and the calculation effort. Therefore, the estimators under comparison were tested by varying the time segment length starting from 5 minutes until 40 minutes with a step of 5minutes. For each time segment length, different numbers of time lags taken from the correlation functions were tried. This leads to different spectra resolutions. For each time segment, the different numbers of points taken from the correlation functions are 128, 256, 512, 1024, 2048 and 3075, which leads to a frequency resolution between 0.0984 and 0.0041Hz. Consequently, for each time segment and number of points combination, the stabilization diagram was analyzed to select the stable pole of the 1st FA mode at the vicinity of the dominant peak. This was done for each estimator under comparison. In this study, we will take the values of the natural frequency and damping ratio estimated from the previous sections as a reference while taking into account that the modal parameters (especially the damping parameter) are highly sensitive to the environmental or operational factors. Therefore, the following paragraphs will discuss the robustness of each estimator to estimate the resonance frequency and damping ratio with varying the time record length and the number of points taken from the correlation functions. Figure 7 shows the estimated 1st FA mode resonance frequency and damping ratio by each estimator for different time record lengths and different number of points taken from the correlation functions. In general, all the estimators under test have a convergence trend with increasing the time record length and this for both the frequency and damping estimates. They converge to a value around 0.358 Hz for the frequency and 1% for the damping ratio. Increasing the time record length makes the estimates obtained from each case of the different number of points taken from the correlation functions to be more clustered around the convergent value. This can be seen clearly from Figure 8, which shows the mean value together with its interval of variation for the frequency and the damping ratio plotted against the time record length.

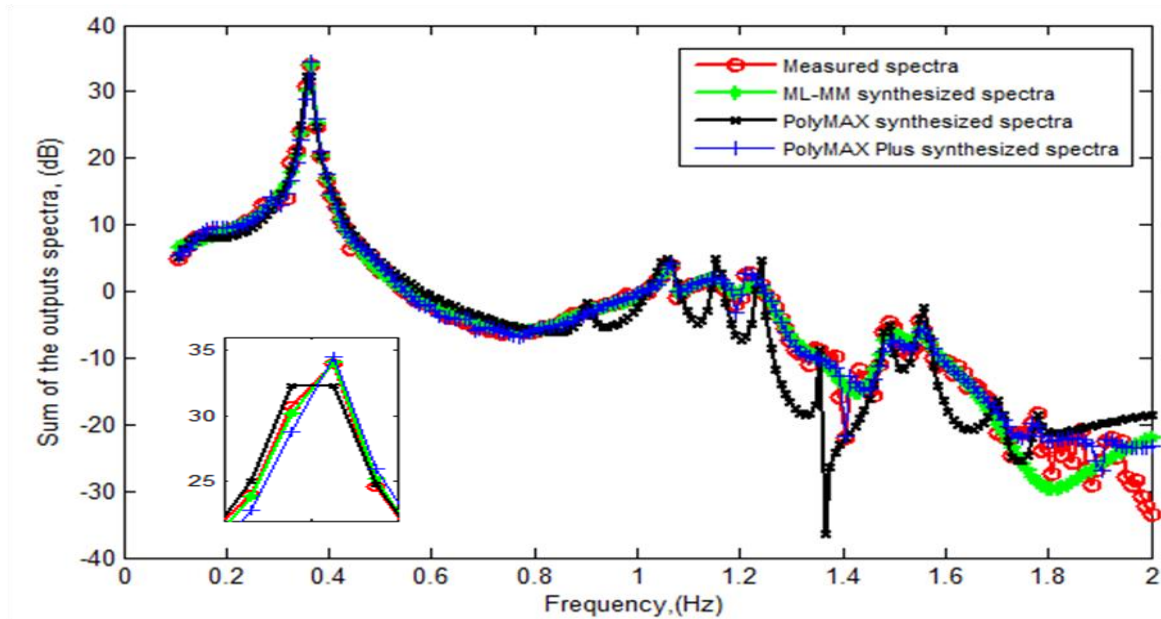


Figure 6: Sum of measured spectra and sum of synthesized spectra by different estimators

The shown mean value in Figure 8 is calculated over the different number of points taken from the correlation function at a constant time record length. From this figure, for all the estimators under test, increasing the time record length leads to decreasing the interval of variation of the mean value. This means that the dependency of the estimates on the number of points taken from the correlation functions decrease. This can be explained by the fact that the use of longer time record permits the development of more averages which minimize the noise effects on the tail of the correlation. In Figure 8, comparing the estimators to each other, one can note that the PolyMAX Plus and the ML-MM approaches compared to the PolyMAX approach are more robust to changing the number of points taken from the correlation functions (i.e. they give smaller error bars) and this is for the frequency estimate as well as for the damping estimate.

Figure 9 shows the mean value together with its interval of variation plotted against the number of points taken from the correlation functions. This mean value is calculated over the different time record lengths at a constant number of points. In this figure, one can note that the plotted error bars for the PolyMAX Plus and the ML-MM approaches are smaller than the ones by the PolyMAX approach. This means that the PolyMAX Plus and ML-MM approaches compared to the PolyMAX approach are more robust to varying the time record length and hence more robust to the variation of the environmental conditions. In addition, Figure 9 shows that taking a very low number of points from the correlation functions leads to frequency and damping estimates with a higher interval of variation (i.e. the estimates are highly fluctuating with the time record length variation). Increasing the number of points to 256, 512, and 1024 points leads to frequency and damping estimates with a lower interval of variation compared to the 128 points case. It is known that taking long correlation functions (e.g. taking 2048 and 3072 points), especially with a short time data set, the noise effects increase and the information about the vibration modes decreases. However, It can be noted from Figure 9 that by taking 3072 points the PolyMAX Plus and ML-MM approaches still give frequency and damping estimates with a lower interval of variation compared to the PolyMAX approach. From Figure 9, it can be seen that 2048 or 3072 points PolyMAX approach gives a damping ratio with a higher interval of variation, which can be explained by the fact that going further to the correlation tail the noise affects the performance of the PolyMAX approach especially with a time record length shorter than 20 minutes. In the same figure, with number of points 3072, the mean value of the damping estimate by PolyMAX Plus and ML-MM approach is lower than 1 % but with a lower interval of variation compared to PolyMAX approach. To sum up, these analyses show that concerning the number of points taken from the correlation functions, 256, 512, and 1024 are good choice for all the three estimators under test. Concerning the time record length, it seems from Figure 8 that the three estimators converge to a frequency estimate at 0.358 Hz at a time record length of 20 minutes.

Concerning the damping estimate, the ML-MM approach converges to a value around 1% at a time record length of 25 minutes, the PolyMAX Plus converges to that value at a time record length of 35 minutes and the PolyMAX has not a convergence where its damping estimate fluctuates around 1% with changing the time record length. So, it can be noted from the results shown in Figure 8 and Figure 9 that the PolyMAX Plus and ML-MM approaches compared to the PolyMAX are robust to the variation in the correlation function length and the time segment length and hence with the environmental factors variations. Taking a 40 minutes time record and 1024 points from the calculated correlation functions, the PolyMAX, PolyMAX Plus, and ML-MM approaches give a damping estimate for the 1st FA mode of 1.04, 1.01, and 1.05 respectively. It can be seen that there is a good correspondence between these values and the values obtained from the overspeed stop test dataset analysis (i.e. section 3 and 4.1).

5 Conclusions

In this contribution, the applicability of three modal parameter estimators is investigated to estimate the damping of the fundamental mode of an offshore wind turbine using outputs-only data. The used estimators, PolyMAX, PolyMAX Plus and ML-MM, are frequency-domain estimators. The damping ratio was estimated using two different data sets. The first data set was a free decay measurement obtained during an overspeed stop test. On this data set, we applied the exponential decay fitting method using different band-pass filters and compared the results with the results obtained from different frequency-domain estimators. The second data set is a 40 minutes acceleration response measured during ambient excitations. It was shown that the damping estimates for all the estimators under comparison using the overspeed test data set are in a good agreement with the ones obtained from the exponential decay fitting method. The good fitting between the measured and synthesized spectra by the PolyMAX Plus and the ML-MM approaches confirms the accuracy of their damping estimates. The results from the ambient test analysis show that for all the estimators under comparison, taking a longer time record length improves the frequency and damping estimate. the PolyMAX Plus and the ML-MM approaches are more robust than PolyMAX approach to varying the pre-processing parameters (i.e. time segment length and the number of points taken from the correlation functions). Taking a long correlation function is not recommended especially not when you have a short time data set (e.g., 256, 512, and 1024 are good choices for the structure under test). The results obtained in this contribution are in good agreement with GL recommendations for additional offshore damping for piled support-structures [17]. The three frequency-domain estimators, which have been tested in this contribution, are originally designed to start from frequency response functions data without taking into account all the problems associated with the operational OWT mentioned in [18]. So, the results presented in this paper will be compared in the near future with some other techniques, which start directly from the measured input-output data instead of the averaged spectra and take into account the transient and unmeasured forces effects [19, 20].

Acknowledgement

This research has been performed in the framework of the Offshore Infrastructure Project (<http://www.owi-lab.be>) the authors also acknowledge the Fund for Scientific Research – Flanders (FWO). The short-term measurement tests were initiated by the engineers of NorthWind NV. They also supplied all relevant operational and structural data, which has been used for the analysis. The authors also gratefully thank the people of Belwind NV for their support before, during and after the installation of the measurement equipment.

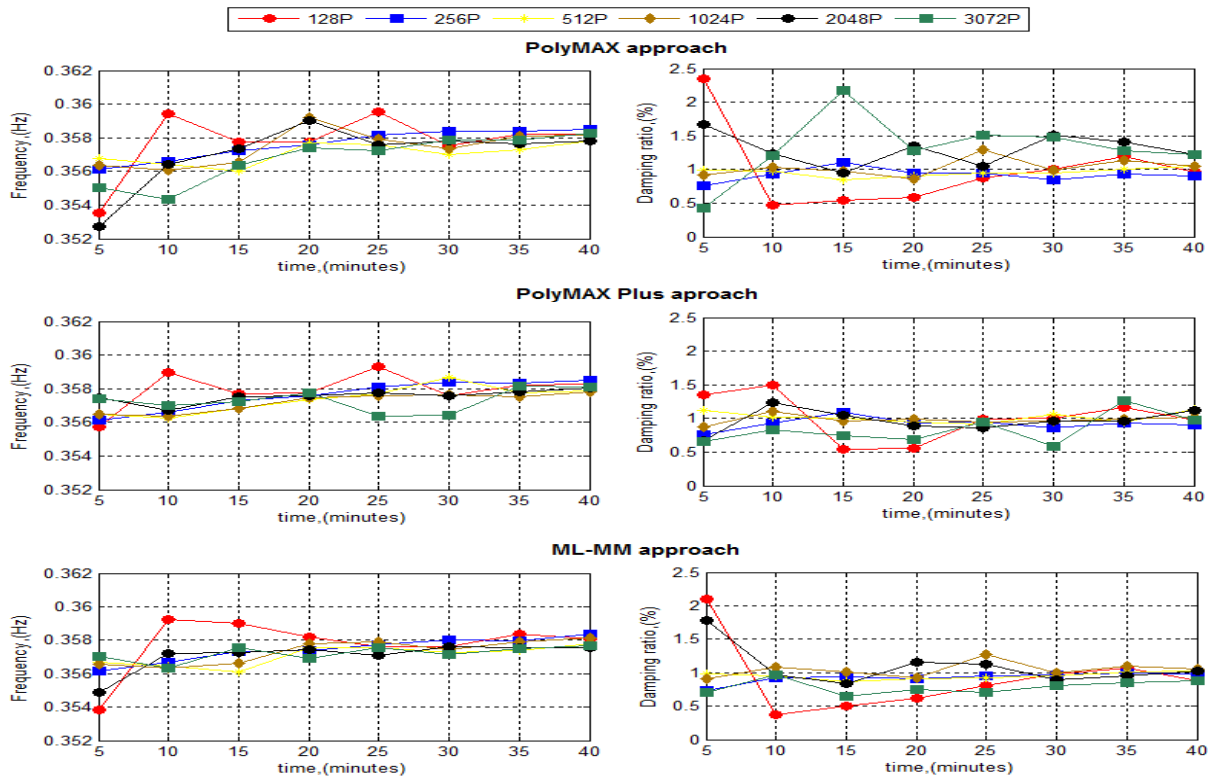


Figure 7: The estimated natural frequency and damping ratio of the 1st FA mode from ambient vibration test at different time and different number of points taken from the correlation functions

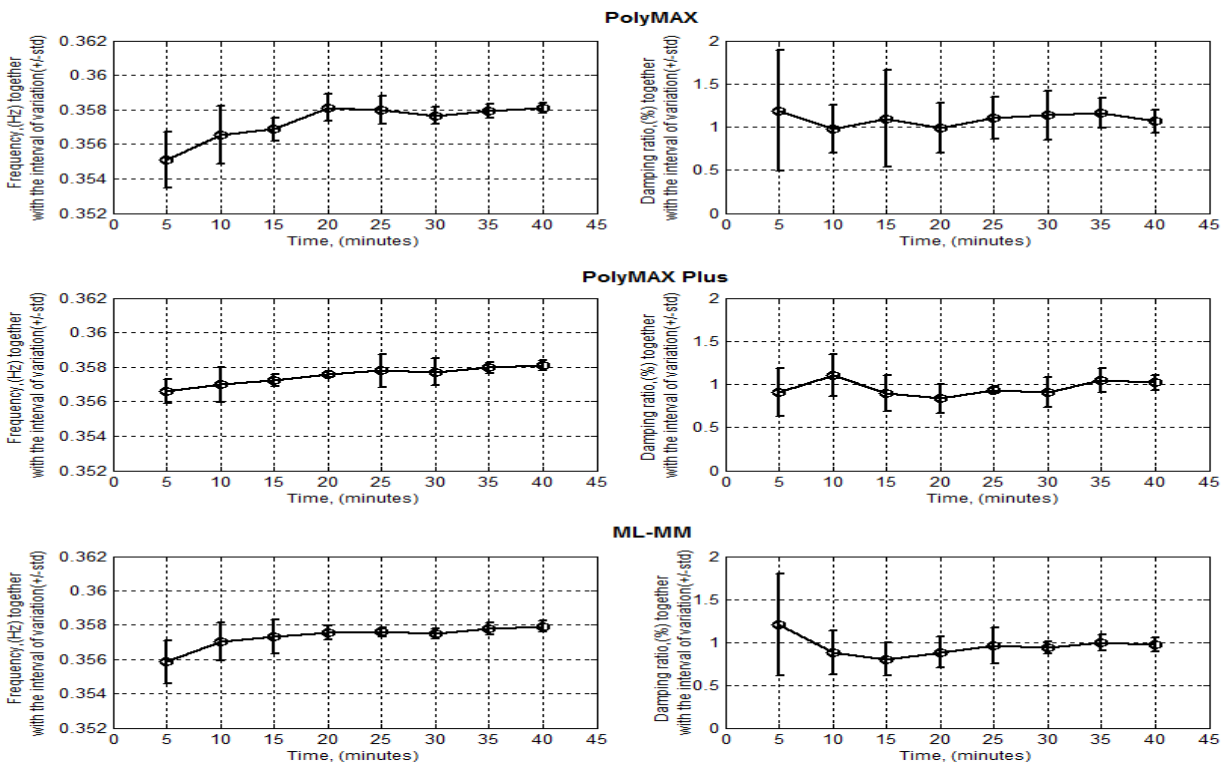


Figure 8: The estimated resonance frequency and the damping ratio of the 1st FA mode: Mean value over the different number of points taken from the correlation functions together with its interval of variation (mean ± std)

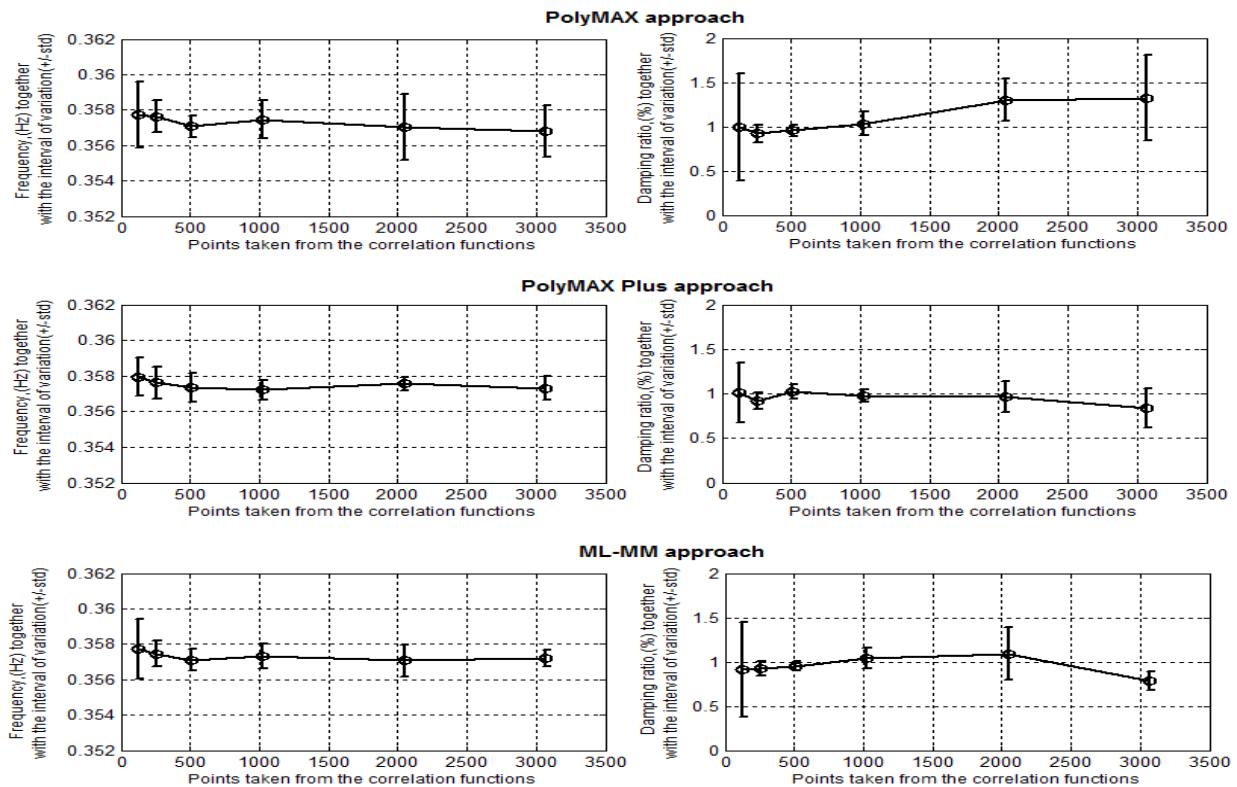


Figure 9: The estimated resonance frequency and the damping ratio of the 1st FA mode: Mean value over the different time segment lengths together with its interval of variation (mean \pm std)

References

- [1] M. Elkafafy, P. Guillaume, B. Peeters, F. Marra and G. Coppotelli, "Advanced frequency domain modal analysis for dealing with measurement noise and parameter uncertainty," in *Proceeding of IMAC-XXX*, Jacksonville, FL, USA, 2012.
- [2] M. Elkafafy, P. Guillaume, T. De Troyer and B. Peeters, "A frequency-Domain Maximum Likelihood Implementation using the modal model formulation," in *Proceeding of the 16th IFAC Symposium on System Identification*, Brussels, 2012.
- [3] Y. Liao and V. Wells, "Modal parameter identification using the log decrement method and band-pass filters," *Journal of Sound and Vibration*, vol. 330, pp. 5014-5023, 2011.
- [4] L. Cremer, M. Heckl and E.E. Ungar, *Structure-Borne Sound*, third ed. ed., Berlin: Springer, 2005.
- [5] H. Van der Auweraer, P. Guillaume, P. Verboven and S. Vanlanduit, "Application of a fast stabilization frequency domain parameter estimation method," *Journal of Dynamic Systems, Measurements and Control*, vol. 123, no. 4, pp. 651-658, 2001.
- [6] P. Guillaume, P. Verboven, S. Vanlanduit, H. Van der Auweraer, and B. Peeters, "A poly-reference implementation of the least-squares complex frequency domain estimator," in *Proceeding of the 21th International Modal Analysis Conference (IMAC)*, Kissimmee, FL, USA, 2003.
- [7] T. De Troyer, P. Guillaume, G. Steenackers, "Fast calculation of confidence intervals on parameters estimate of least squares frequency domain estimator," *Mechanical System and Signal processing*, vol. 23, pp. 1423-1433, 2009.
- [8] B. Peeters, H. Van der Auweraer, F. Vanhollenbeke and P. Guillaume, "Operational modal analysis for

- estimating the dynamic properties of a stadium structure during a football game," *Shock and Vibration*, vol. 14, pp. 283-303, 2007.
- [9] C. Devriendt and P. Guillaume, "Identification of modal parameters from transmissibility measurements," *Journal of Sound and Vibration*, vol. 314, no. (1-2), pp. 343-356, 2008.
- [10] C. Devriendt, G. De Sitter, S. Vanlanduit and P. Guillaume, "Operational modal analysis in the presence of harmonic excitations by the use of transmissibility measurements," *Mechanical system and signal processing*, vol. 23, no. 3, pp. 621-635, 2009.
- [11] P. Guillaume, P. Verboven, and S. Vanlanduit, "Frequency-domain maximum likelihood identification of modal parameters with confidence intervals," in *In Proceedings of the 23rd International Seminar on Modal Analysis*, Leuven, Belgium, 1998.
- [12] L. Hermans, H. Van der Auweraer and P. Guillaume, "A frequency-domain maximum likelihood approach for the extraction of modal parameters from output-only data," in *In Proceedings of the 23rd International Seminar of Modal Analysis*, Leuven, Belgium, 1998.
- [13] R. Pintelon, P. Guillaume, and J. Schoukens, "Uncertainty calculation in (Operational) modal analysis," *Mechanical System and Signal Processing*, vol. 21, pp. 2359-2373, 2007.
- [14] B. Cauberghe, "Applied frequency-domain system identification in the field of experimental and operational modal analysis," PhD thesis, Vrije Universiteit Brussel, 2004.
- [15] P. Guillaume, R. Pintelon and J. Schoukens, "Robust parameteric transfer function estimation using complex logarithmic frequency response data," *IEEE Transactions on Automatic Control*, vol. 40, no. 7, pp. 1180-1190, 1995.
- [16] J. Schoukens and R. Pintelon, and J. Renneboog, "A maximum likelihood estimator for linear and nonlinear system- A practical application of estimation techniques in measurements problems," *IEEE Transactions on Instrumentation and Measurement*, vol. 37, no. 1, pp. 10-17, 1988.
- [17] "Overall Damping for Piled Offshore Support Structures, Guideline for the Certification of Offshore Wind Turbines," Germanischer Lloyd, WindEnergie, Edition 2005.
- [18] D. Tcherniak, S. Chauhan and M. H. Hansen, "Applicability limits of Operational Modal analysis to operational wind turbines," in *In Proceedings of IMAC XXVIII*, Jacksonville, FL, USA, 2010.
- [19] B. Cauberghe, P. Guillaume, P. Verboven, and E. Parloo, "Identification of modal parameters including unmeasured forces and transient effects," *Journal of Sound and Vibration*, vol. 265, no. 3, pp. 609-625, 2003.
- [20] P. Verboven, B. Cauberghe, P. Guillaume, S. Vanlanduit, and E. Parloo, "Modal parameter estimation from input-output Fourier data using frequency-domain maximum likelihood identification," *Journal of Sound and Vibration*, vol. 276, no. 3-5, pp. 957-979, 2004.

